ADVANCED MATERIALS
www.advmat.de

Superconducting Nanowires Fabricated Using Molecular Templates

By *Alexey Bezryadin** and *Paul M. Goldbart**

The application of single molecules as templates for nanodevices is a promising direction for nanotechnology. We use suspended deoxyribonucleic acid molecules or single-walled carbon nanotubes as templates for fabricating superconducting devices and then study these devices at cryogenic temperatures. Because the resulting nanowires are extremely thin, comparable in diameter to the templating molecule itself, their electronic state is highly susceptible to thermal fluctuations. The most important family of these fluctuations are the collective ones, which take the form of Little's phase slips or ruptures of the many-electron organization. These phase slips break the quantum coherence of the superconducting condensate and render the wire slightly resistive (i.e., not fully superconducting), even at temperatures substantially lower than the critical temperature of the superconducting transition. At low temperatures, for which the thermal fluctuations are weak, we observe the effects of quantum fluctuations, which lead to the phenomenon of macroscopic quantum tunneling. The modern fabrication method of molecular templating, reviewed here, can be readily implemented to synthesize nanowires from other materials, such as normal metals, ferromagnetic alloys, and semiconductors.

1. Introduction

Molecular templating (MT)[1] offers the possibility of fabricating homogeneous wires, which can be made very short (as short as ~30 nm)[2] and very thin, viz. as thin as ~5 nm or possibly even thinner.[1,3–6] The MT technique involves the sputter-deposition of a thin metallic film over suspended (and dried) DNA molecules[4,7,8] or a carbon nanotubes.[1,3,5] The results published so far indicate that not all metals form homogeneous nanowires when deposited on the surface of a carbon nanotube. Amorphous alloys, such as Mo_xGe_{1-x}, provide wires having a high degree of homogeneity.[1,6] For elemental metals the general tendency is to form disconnected grains when deposited on a carbon nanotube.[3] On the other hand, some elemental metals, such as Nb,[5,9] amorphous Os,[5] and Ti,[3] exhibit strong adhesion to the nanotube. These metals can be used as "sticking" layers for other metals.[3] Thus, in the MT method the choice of the material determines the morphology of the resulting nanowire. In this Research News article we focus on wires fabricated by a sputter-deposition of $Mo_{79}Ge_{21}$ films[10,11] over suspended carbon nanotubes. The elemental compositions of the alloy were as indicated (or similar to this), and were optimized with the goal of obtaining the highest critical temperature for the superconducting transition. This particular alloy shows an excellent adhesion to nanotubes (and to DNA also). The MT method also has the virtue of creating wires that are seamlessly connected to the measurement leads. Thus, the MT technique provides an efficient solution to the general problem of making good electrical contact to the nanowires under investigation.

Nanowire devices have been used to study quantum coherence and decoherence effects in 1D superconductors. A single-wire device consists of two coplanar superconducting films (to be called "electrodes" or "thin-film electrodes"), connected electrically to each other through just one individual superconducting nanowire. The supercurrent flowing from one electrode to the other through the nanowire is proportional to the difference of the phases of the condensate wave functions in each of the electrodes. If the wave function in the wire is coherent (i.e., the phase difference evolves in agreement with the Schrödineger equation), then a supercurrent can flow with zero voltage applied. On the other hand, if the rate of occurrence of decoherence events (i.e., Little's phase slips (LPSs))[12] is not zero, a proportional voltage occurs between the electrodes. Thus, by measuring the voltage (with a weak constant current being applied through the wire) we determine the rate at which the phase-coherence-breaking phase slips occur. We find that at low bias-current this rate of phase slips follows the Arrhenius thermal-activation law. Similar results have recently been obtained in experiments on thin wires fabricated from high-temperature superconductor materials.[13] In our experiments, no signatures of quantum

[*] Prof. A. Bezryadin
Frederick Seitz Materials Research Laboratory
Department of Physics
University of Illinois at Urbana-Champaign
Urbana, Illinois 61801 (USA)
E-mail: bezryadi@illinois.edu
Prof. P. M. Goldbart
Frederick Seitz Materials Research Laboratory
Institute for Condensed Matter Theory
Department of Physics
University of Illinois at Urbana-Champaign
Urbana, Illinois 61801 (USA)
E-mail: goldbart@illinois.edu

DOI: 10.1002/adma.200904353

tunneling of the phase slips was observed in our short wires at *low* bias-currents. However, at *high* bias-currents, i.e., at currents close to the critical current of the nanowire, we do observe a clear signature of quantum phase slips (QPSs), namely, strong fluctuations in the currents at which switching to a resistive state occurs.[14]

2. Fabrication of Nanowires Using Molecular Templates

The technique of MT[1] can be used to fabricate homogeneous metallic wires with ultrasmall dimensions, i.e., of diameters significantly less than ~10 nm and lengths as small as ~30 nm. One important advantage of MT is that, as produced, the nanowires are seamlessly connected to metallic electrodes, thus ideal for transport measurements of various types. Another advantage is that the technique can be generalized to various materials and also to a range of geometries, if substrate molecules (or molecular assemblies) of the desired geometry can be synthesized and obtained in a suspended state.

In the MT method (see Fig. 1), fabrication starts with a Si (100) wafer covered with a 500-nm-thick layer of SiO_2 (including a 100-nm-thick film of "dry oxide" and a 400-nm-thick film of "wet oxide") and a 60-nm-thick film of low-stress SiN deposited by low-pressure chemical vapor deposition (LPCVD) over the oxide layer.[15] In the next fabrication step, a narrow (~100 nm) and long (~5 mm) trench is defined in the top layer of SiN using electron beam (e-beam) lithography with PMMA resist, followed by reactive ion etching using SF_6 plasma. A focused ion beam (FIB) can be used instead of e-beam lithography to form the trench. An undercut (see Fig. 1) surrounding the trench is then formed by wet etching in 50% HF for ~10 s. A less concentrated HF solution can also be used, but the etching time should then be increased. The undercut develops because the etching rate of the oxide is much larger than the etching rate of the nitride. We typically try to make the undercut to be about 300 nm in width, on each side of the trench. The undercut is very important for proper device operation, as it ensures that the electrodes formed in the subsequent metal sputtering step are electrically disconnected everywhere except through the nanowire. The deposition of molecules is done from the liquid phase, which can be a solution of fluorinated nanotubes in isopropanol, a suspension of regular nanotubes in dichloroethane, or a water solution containing λ-DNA molecules. The solvent can either be removed by blowing dry nitrogen gas over the sample or, in the case of DNA deposition, by evaporation in a vacuum-desiccator.

After the solvent is removed, a metallic film is sputter-deposited over the entire sample. For each sample only one sputtering run is carried out, in which the wire and the leads are produced simultaneously. After the sputtering, each molecule suspended over the trench has become coated with metal, and thus is transformed into a very thin metallic nanowire. After the

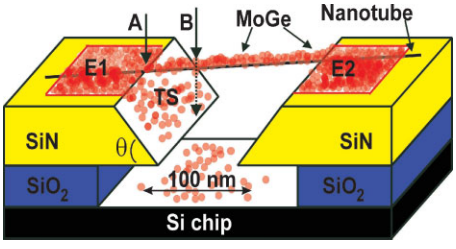

Figure 1. Schematic image of the principle of MT.[6] Here, a nanotube is positioned over a narrow (~100 nm) trench etched into the top SiN layer (yellow). The layer of SiO_2, which is available directly under the SiN film is used to create an undercut via HF wet etching. In order to make the the sample out of a metallic nanowire, the desired metal—typically $Mo_{79}Ge_{21}$ or Nb—is sputter-deposited over the entire surface of the Si chip, including the molecule suspended over the trench. As the sputtered metal atoms (red circles) stick to the suspended nanotube, a metallic nanowire forms on the surface of the nanotube. The electrodes, which are thin MoGe films, usually ~15 μm wide, are marked E1 and E2. In a real sample, the electrode smoothly transition into larger-area contact pads, with at least two pads on each side of the trench. The contact pads are not shown here. The segment of the wire located between arrows A and B is suspended over the tilted sides (TS) of the trench, and therefore it appears as a "white spot" when imaged using SEM.

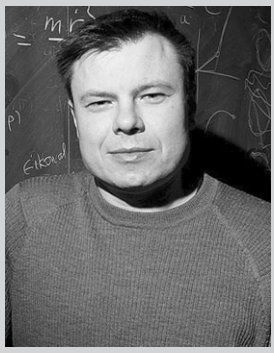

Alexey Bezryadin received his B.Sc. and M.Sc. degrees in Physics and Applied Mathematics from the Moscow Institute of Physics and Technology, Russia, in 1990. He received his doctorate in Physics from the Joseph Fourier University in Grenoble, France, in 1995, after which he was a postdoctoral researcher at Delft University of Technology in the Netherlands (1995–1997) and at Harvard University, USA (1997–2000). He joined the Physics Department of the University of Illinois at Urbana-Champaign, USA, in 2000, where he currently holds the positions of Associate Professor of Physics and Research Professor in the Frederick Seitz Materials Research Laboratory.

Paul Goldbart received his B.A. degree in Physics and Theoretical Physics from the University of Cambridge, UK, in 1981, and his M.Sc. degree in Physics from the University of California–Los Angeles, USA, in 1982. He received his doctorate in Physics from Imperial College of Science and Technology, University of London, UK, in 1985. In 1985 he joined the Department of Physics at the University of Illinois at Urbana-Champaign, USA as a postdoctoral researcher, where he became Assistant Professor in 1987. He currently holds the positions of Professor of Physics, Director of the Institute for Condensed Matter Theory, and Research Professor in the Frederick Seitz Materials Research Laboratory.

sputter-deposition step, the Si chip is examined using scanning electron microscopy (SEM), and a wire with no visible defects is selected. Under ''visible defects'' we understand interruption and/or constrictions, or other imperfections, which can be seen on SEM images of the examined nanowire. After a solitary and defect-free wire is found, its position is determined with respect to a periodic set of markers located near and along the trench. Then, the sample is spin-coated with a photoresist and subjected to photolithography, while the optical mask alignment is guided by the markers. The markers, which are simply numbers etched into the SiN film, have typical dimensions of about 5–10 μm, so they are clearly visible in the optical microscope used to align the photomask. The markers are spaced periodically along the trench with a step of ~20 μm. Making samples with just one wire connecting the electrodes is possible because the concentration of wires can be made sufficiently low, typically one per every ~100 μm of the trench length, while the width of the electrodes, defined by the photomask, is usually five to ten times smaller than this.

As a result of photolithography a sample is obtained that has contact pads connected to ~15-μm-wide electrodes, which approach the trench from opposite sides, the wire serving as a weak electrical link bridging the trench and connecting the electrodes to one other.

SEM imaging shows that MT-produced nanowires are continuous and homogeneous (Fig. 2). Some apparent surface roughness can be attributed to the amorphous structure of the wire (meaning a random arrangement of atoms) and to oxidation of its surface, as the nanowires are exposed to air during the fabrication steps. Imaging with transmission electron microscopy (TEM) confirms that the wires are structurally homogeneous and amorphous.

3. Electrical Transport Measurements

The sample is biased with an AC current at a frequency of ~11 Hz and amplitude in the range 1–10 nA. The current bias is achieved by using an ultralow-distortion function generator (Stanford Research Systems DS 360). The voltage from the generator is applied to the sample through a standard resistor with a value of ~1 MΩ, which is much larger than the typical resistance of the sample and the leads connected to the sample (which is ~1–10 kΩ). Thus, the current through the sample, connected in series with the standard resistor, is mostly determined by the value of the resistor. This current is recorded, as a function of time, by measuring the voltage across the standard resistor (and dividing the measured voltage by the value of the standard resistor). The voltage on the superconducting electrodes is also measured (with a separate pair of leads) and recoded as a function of time. Both measurements are carried out using battery-powered preamps (either Princeton Applied Research model 113 or Stanford Research Systems model SR 560). After one period of the sinusoidally time-dependent bias current is completed, the recorded voltage V is plotted as a function of current I. Thus, the $V(I)$ curve is obtained and is plotted on the screen of a computer using LabVIEW software. In order to determine the linear resistance of the sample (also called zero-bias resistance), the current-bias amplitude is chosen to be small enough that the $V(I)$ curve is linear. Then, the best linear fit to the $V(I)$ curve is found using LabVIEW functions. The slope of the linear fit is defined to be the resistance R of the sample.

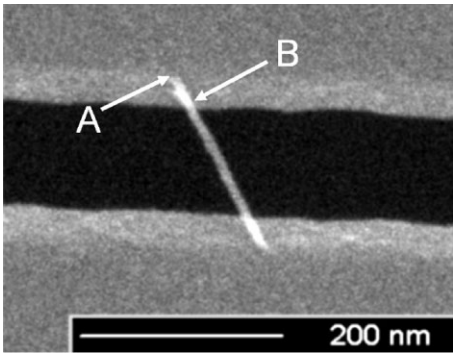

Figure 2. A SEM image of a MoGe nanowire (gray) suspended over a trench (black) and seamlessly connecting to two MoGe electrodes (gray areas on the top and on the bottom).[6] The white spots are visible on both sides of the wire, indicating that the wire is straight and well suspended. The beginning and end of one of the white spots are marked by arrows A and B, corresponding to the A and B arrows of Figure 1.

At low-enough temperatures ($\leq$ 1 K), typical nanowires, if they are not too thin, show pronounced signs of superconductivity. The wire has to be ''not too thin'' because wires that are thinner than some length- and material-dependent critical diameter do not exhibit any signs of superconductivity but, rather, can be characterized as insulating wires.[2] Here, we discuss only superconducting wires, but not insulating ones. The resistance R of the superconducitng wires becomes immeasurably small at low temperatures. For the type of measurement outlined above, the lowest value of R that can be measured is roughly 1 Ω. This lowest value is called the ''noise floor'' of the setup. As the temperature of the sample is reduced below a certain value, R drops below the noise floor and cannot be measured. At such low temperatures, we perform a complementary measurement, namely, a measurement of the switching current I_{SW}. To do this, the bias current is slowly increased until a sharp, jump-wise increase in R is observed. In such jumps, R increases from apparently zero up to the normal resistance of the wire R_N. The current at which the jump occurs is called I_{SW}. After the switching event, the wire is in the normal state, due to excessive Joule heating. To return the wire to the superconducting state, the bias current has to be reduced considerably. The current at which the wire switches back to the superconducting regime is called the ''retrapping current'' I_R.

A typical dependence of the sample resistance on temperature $R(T)$ is shown in Figure 3. Due to the fact that the wire is connected in series with the thin-film electrodes, two resistive transitions are observed. At ~6 K the electrodes E1 and E2 (see Fig. 3) become superconducting. Thus, below this temperature the measured resistance is entirely due to the nanowire. The second transition (at ~3.5 K) is due to the nanowire losing its resistance. In all measured samples it was found that wires made of MoGe alloy show a lower critical temperature, compared to films of the same thickness. This reduction (in the wires compared to thin films of the same thickness) of the critical temperature may be due to reduction of the screening of the Coulomb repulsion between the electrons,[16]

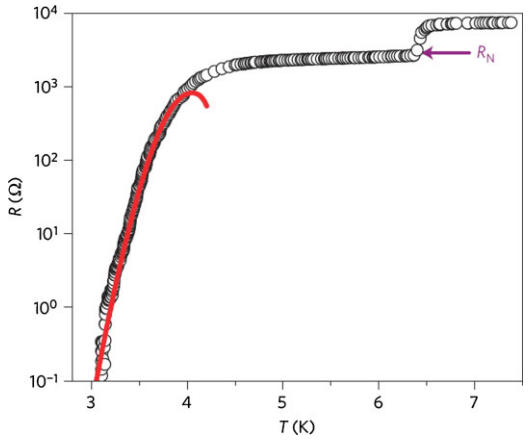

Figure 3. An $R(T)$ curve for a typical sample involving a single MoGe nanowire.[14] The template used to make the wire was a fluorinated carbon nanotube. The sample resistance is plotted versus temperature in a log-linear format. The first resistive transition, occurring at ~6.0 K, is due to the superconducting transition taking place in the film electrodes that are linked to the wire. The second apparent transition, at ~4 K, corresponds to the occurrence of a superconducting behavior in the nanowire. The negative curvature of the low-temperature part of the curve indicates that the wire resistance drops, with cooling, at a rate that is faster than exponential, i.e., in accordance with Arrhenius activation law, with the barrier that depends on temperature (the red fit).

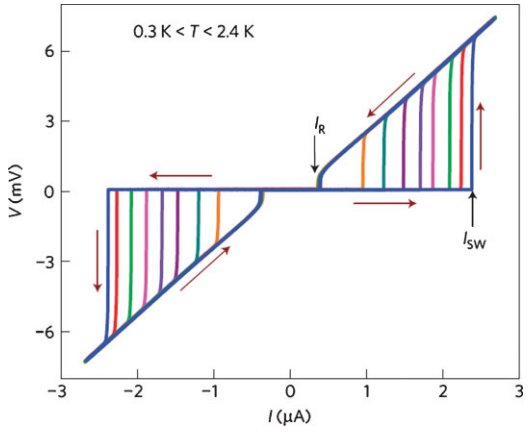

Figure 4. A series of voltage-versus-current curves $V(I)$ of a typical sample involving a single MoGe nanowire, measured at various temperatures.[14] The switching current I_{SW} and the retrapping current I_R are indicated for the curve measured at 0.3 K. The corresponding temperatures are 0.3 K (corresponding to the highest I_{SW}), 0.6, 0.9, 1.2, 1.5, 1.8, 2.1, 2.4 K. As the temperature is increased the value of I_{SW} decreases. This sample was synthesized using a fluorinated carbon nanotube as template molecule.

as well as due to the obvious fact that the wire oxidizes (when exposed to air) from all sides, while the film oxidizes only at its top surface. We define the normal-state resistance of the wire R_N to be the sample resistance measured immediately below the temperature at which the leads become superconducting, as shown by the arrows in Figure 3.

Voltage–current characteristics, measured at various temperatures, of a typical sample with a single nanowire are shown in Figure 4. The larger arrows show the directions of sweeping of the bias current. The switching current I_{SW} is marked by the upward arrow. When the bias current is increased to the value of I_{SW} the wire switches abruptly to a resistive state, which is, in fact, the normal state of the wire, maintained by Joule heating.[17] The retrapping current I_R is marked by the downward arrow. The transition at I_R is also abrupt. It is clear from the graph that the switching current is very sensitive to changes in temperature. As the temperature is increased, the I_{SW} decreases significantly. On the contrary, the I_R is almost independent of temperature, until the temperature reaches a higher value of $T \sim 2$ K, at which a noticeable decrease in I_R is found with increasing the temperature.

4. Little's Phase Slip as a Mechanism of Supercurrent Dissipation

Consider a model: a thin superconducting wire forming a closed loop.[12] Suppose the initial state of the system is such that the supercurrent I_S in the loop is such that $0 < I_S < I_C$, where I_C is the critical current of the wire, i.e., the current that is sufficient to destroy superconductivity. If fluctuations are weak, such a state of the system would persist indefinitely. The analysis by Little[12] shows that only strong fluctuations, viz., those that bring the order parameter to zero at some spot along the wire, can cause the supercurrent to decay.

The reason is the following. In a superconducting wire, $I_S \sim \phi/L$, where L is the wire length (or the loop length) and ϕ is the difference in the phase of the complex-valued wavefunction describing the superconducting condensate. The phase difference is taken between the ends of the wire, if the wire is connected to superconducting electrodes. In Little's model, the wire forms a loop, and thererfore ϕ stands for the phase accumulated along the closed path coinciding with the the loop itself. As the wavefunction must be single-valued, the phase difference around a closed loop is always $\phi = 2\pi n$. Here, n is an integer that sometimes is called the "vorticity" of the state and can be regarded as the number of coreless vortices trapped within the loop (take notice: we are assuming here that the magnetic field is zero everywhere). The fact is that unless n is changed the current I_S cannot change, because $I_S = \text{const} \times \phi = \text{const} \times n$. Little's topological analysis of the loop model shows that the phase difference ϕ can only change if a strong and rare fluctuation occurs, such that it brings the amplitude of the complex wavefunction describing the condensate (sometimes called superconducting "order parameter") to zero at some point on the wire. If this happens, the phase can change by 2π (or integer multiples of it.) One way to understand this is to realize that without a magnetic field the supercurrent in the loop is proportional to the number of coreless vortices n trapped within the loop. To reduce the value of the supercurrent a vortex must be expelled from the loop. To exit the loop, the core of a vortex must cross the loop at some point. Thus, there is an energy barrier for such process, which is roughly equal to the energy of the vortex core positioned somewhere on the wire that forms the loop. The vortex core is simply a normal (i.e., non-superconducting) region of size roughly the superconducting coherence length $\xi(T)$. At low temperatures, the free energy of the superconducting state is lower than the free energy of the normal state, and the difference is given by the so-called condensation-energy density $H_c^2/8\pi$.

Thus, the energy barrier for such vortex-crossing process ΔF can be estimated via $\Delta F \sim A\xi H_c^2/8\pi$, where $A\xi$ is the volume of the normal region associated with the normal core position on the wire, the cross-sectional area of which is A, and H_c is the thermodynamic critical field. The event when a vortex trapped in the the loop crosses the wire (that makes the loop) and escapes to infinity is an example of LPS. The essential properties of LPS are: (i) LPS can only occur if the order parameter (represented by the radius of the order-parameter spiral) reaches zero (at least instantaneously), and (ii) LPS causes a change of the phase-difference by 2π, which precisely means that the spiral, representing the order parameter in the Argand diagram, loses one turn.

The rate of thermally activated phase slips (TAPSs), Γ_{TAPS}, is governed by the Arrhenius activation law and can be written as $\Gamma_{\mathrm{TAPS}} = \Omega \exp(-\Delta F/k_B T)$. Here, Ω is an effective attempt frequency, which was estimated rigorously only for temperatures near the critical temperature.[18] At low temperatures, when thermal fluctuations are weak and the associated rate of phase slips is low, quantum fluctuations might play a role and allow the vortices trapped in a loop to escape by tunneling. Thus the supercurrent would decay due to QPS. The rate of QPS is determined by the quantum action of the vortex core crossing the wire and can be roughly estimated, following the Giordano model,[19] as $\Gamma_{\mathrm{QPS}} = \Omega_{\mathrm{QPS}} \exp(-\Delta F/k_B T_Q)$, where Ω_{QPS} represent some effective attempt frequency of the quantum fluctuations of the order parameter amplitude and T_Q is a phenomenological parameter (quantum temperature) defining the strength of quantum fluctuations.

One of the goals of developing the theory of phase slips is to be able to predict the temperature dependence of the resistance of a thin wire, $R(T)$, such as those shown in Figure 3. The main hypothesis needed for the calculation is that even if the wire is not forming the loop but, instead, it is connected to some external leads, which are used to inject the current into the wire, the resistance of the wire would be determined exclusively by the LPS rate (assuming that a dc measurement is considered). A detailed theoretical analysis of such situation was given by Langer and Ambegaokar[20] and by McCumber and Halperin.[18] The corresponding theory is called LAMH theory. This theory does not take into account the possibility of QPS but only treats TAPS.

Below we list the corresponding formulas. Within the LAMH theory the resistance is predicted to be $R_{\mathrm{LAMH}}(T) = R_Q(\hbar\Omega_{\mathrm{TAPS}}/k_B T)\exp(-\Delta F(T)/k_B T)$, where $\hbar = h/2\pi$, h is Planck's constant, k_B is Boltzmann's constant, $\Delta F(T)$ is the temperature-dependent barrier for phase slips, and $R_Q = h/4e^2 = 6.5\ \mathrm{k}\Omega$ is the quantum of resistance (in which $-e$ is the charge of the electron).[21] In the LAMH model, the attempt frequency is given by[18]

$$\Omega_{\mathrm{LAMH}} = (1/\tau_{\mathrm{GL}})(L/\xi(T))\sqrt{\Delta F(T)/k_B T} \quad (1)$$

Here, $\tau_{\mathrm{GL}} = \pi\hbar/8k_B(T_C - T)$ is the so-called Ginzburg–Landau relaxation time. LAMH theory is only valid near T_C, because it is based on time-dependent Ginzburg–Landau theory, which has a narrow range of applicability. By some estimates,[22] it can only be applied in a narrow range, such as $0.90T_C < T < 0.94T_C$.

Thus, it is desirable to have approximations applicable at lower temperatures. These approximations rely on the Arrhenius factor alone, which is correct down to zero temperature, providing that only thermal activation—but not quantum tunneling—of LPS needs to be accounted for (quantum tunneling will be discussed separately, below). An approximate formula for the wire resistance caused by TAPS is $R_{\mathrm{AL}}(T) = R_N \exp(-\Delta F/k_B T)$. It can be referred to as the Arrhenius–Little (AL) formula because the exponential factor is the usual thermal-activation law, analogous to the Arrhenius law, and the prefactor is the normal resistance of the wire. One can argue that such prefactor is reasonable, based on the Little's hypothesis that each phase slip creates a region of size $\xi(T)$ that simply acts as normal metal and has an electrical resistance of $R_N\xi(T)/L$. One needs to take into account the fact that each segment of the wire does not stay normal at all times but, rather, becomes normal only in the rare event that an LPS occurs on the segment under consideration.[23] It should be emphasized that R_{LAMH} and R_{AL} are qualitatively distinct, in the sense that the prefactor of R_{AL} includes the wire's normal resistance, whereas the prefactor of R_{LAMH} is independent of the normal resistance of the wire. Yet, the role played by the prefactor is negligible in all practical cases so that both formulas can be used to fit the experimental $R(T)$ curves. This fact is illustrated in Figure 5, where both types of fit are shown, and both exhibit good agreement with the data. Thus, the LAMH and AL formulas can be used interchangeably to approximate the experimental results. There is some evidence though that the LAMH fit overestimates the critical temperature of the wire.[23]

To complete the list of useful formulas, one needs the expression relating the LPS barrier $\Delta F(T)$ to the critical current of the wire $I_C(T)$, which is[24]

$$\Delta F(T) = \sqrt{6}(\hbar/2e)I_C(T) \quad (2)$$

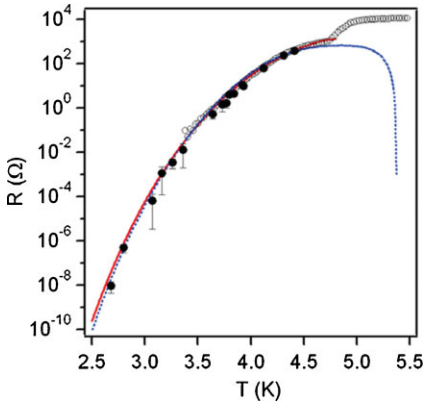

Figure 5. Resistance-versus-temperature curve for a narrow superconducting bridge, the sample B2 from Reference [23]. This samples was fabricated as is illustrated in Figure 1, including metallization with sputtered MoGe, except that instead of a nanotube a SiN bridge was used as a template. Open circles represent direct low-bias transport measurements of the sample resistance. Filled circles represent the resistance determined indirectly, namely, by extrapolating high-bias segments of the nonlinear $V(I)$ curves. The solid (red) and the dashed (blue) curves give the best fits generated by the R_{AL} and R_{LAMH} formulas, respectively. Both models show a good agreement with the data. The downturn of the blue curve, which corresponds to LAMH theory, is an artifact of the theory that is related to the fact that the attempt frequency Ω_{LAMH} goes to zero as $T \rightarrow T_C$.

Another important estimation is the formula

$$\Delta F(0) = 0.83 k_B T_c \left(R_Q / R_N\right)\left(L/\xi(0)\right), \quad (3)$$

which relates the barrier for phase slips to the normal resistance of the wire.[24] Close to T_C the coherence length can be approximated as $\xi(T) = \xi(0)/\sqrt{1 - T/T_C}$, where $\xi(0)$ is the zero temperature coherence length. There is also an expression for the critical current of the wire, applicable at all temperatures, namely, the Bardeen formula,[25]

$$I_C(T) = I_C(0)\left(1 - (T/T_C)^2\right)^{3/2} \quad (4)$$

5. Evidence for Macroscopic Quantum Tunneling

Quantum behavior involving macroscopic degrees of freedom—i.e., physical variables describing large ensembles of particles—represents one of the most exciting fields of modern physics. A simple example of a macroscopic degree of freedom is the position of the center of mass of a large object, say a C_{60} molecule.[26] Initiated by Leggett more than 25 years ago,[27] research on macroscopic quantum tunneling (MQT) has undergone widespread development. Important settings for realizing MQT phenomena include such diverse systems as superconductor–insulator–superconductor (SIS) Josephson junctions,[28] and magnetic nanoparticles.[29]

The recognition of the advantages of quantum computers[30] has motivated the search for viable implementations of quantum bits, or qubits, several of which employ MQT in superconducting systems.[31] Interestingly, it has also been proposed that superconducting nanowires, if they exhibit MQT, could provide a possible setting for realizing novel qubits with improved decoherence properties.[32]

Also, substantial evidence has accumulated to indicate that MQT can occur in thin metallic wires of rather homogeneous cross-section (see Reference [33] and references therein). In nanowires, the MQT phenomenon is referred to as QPSs. The occurrence of QPS implies that the wire is never truly superconducting: its resistance does not approach zero even when the temperature does. Thus, evidence for QPS is usually sought via the observation of a nonzero resistance at temperatures much lower than the critical temperature of the wire. Typically, one concludes that QPS are present if $R(T)$ is flat at low temperatures or if R drops with cooling slower than what might be expected from the thermal activation law $R \sim \exp(-\Delta F/k_B T)$. On the other hand, our *short* wires made of MoGe did show strong evidence in favor of the existence of a true superconducting regime [which is characterized by $R \sim \exp(-\Delta F/k_B T)$],[2] i.e., a regime without QPS. Note that at $T > 0$, the resistance is greater than zero in any model, as some LPS thermal activation is inevitable unless $T = 0$. The question that is not completely clear is whether or not signatures of MQT can be observed in *short* MoGe wires. (Empirically, "short" is defined as being shorter than ~250 nm.)

The possibility of MQT in superconducting junctions having insulating barriers has been clearly demonstrated experimentally (see Reference [34] and references therein). This was achieved by exposing the samples to microwave radiation, and observing the discrete nature of the allowed energy states of the entire device, as one expects for a quantum system. More precisely, the microwaves were able to excite the system from the ground state to the next level, but only if the level spacing was equal to the energy of the photons of the applied radiation. Thus, it was possible to study the discrete energy states. Excitation of the system was detected through the premature switching (due to MQT) of the device from the superconducting to the normal state.

Recent experiments by Sahu et al.[14] give new evidence for MQT in homogeneous superconducting wires. This evidence for MQT is obtained by analyzing switching events, which occur at high bias currents, close to the depairing current. Below, we shall show how a detailed analysis of the statistics of the superconductor-to-normal switching currents can provide an affirmative answer to the question of whether or not QPS can occur in nanowires. The main point of argument is that at low temperatures ($T \sim 300$ mK) the fluctuations of the value of the I_{SW} are much larger than the value expected on the basis of thermal fluctuations, and can be directly linked to QPS, which are a manifestation of quantum fluctuations. Thus, it is found that, although short MoGe wires do not exhibit QPS at low bias-currents, signatures of QPS do appear at high bias-currents near the depairing current, via the statistics of the premature switching events.[21]

5.1. Strong Fluctuations of the Value of the Switching Current

The switching current of a nanowire shows very pronounced fluctuations, much stronger than the instrumental noise.[14] To characterize the fluctuations of I_{SW} quantitatively, the temperature is typically fixed and the $V(I)$ curve is measured ten thousand times. For each $V(I)$ curve, the value of I_{SW} is determined by finding the current at which the voltage exceeded the noise floor (~10 μV) by about one order of magnitude. As the voltage jump at the switching current is very strong, the results are independent on the precise choice of the threshold voltage. The results of such an analysis, for various temperatures, are shown in Figure 6. It can bee seen that, as we increase the value of T (in the interval $0.3\,\mathrm{K} < T < 2.3\,\mathrm{K}$), the distributions of the switching currents become narrower (and correspondingly taller, while the area, which represents the total number of measurements, is the same for all curves). The vertical axis of Figure 6, marked "Count," can be expressed as $\mathrm{Count} = 10^4 P(I_{SW})\Delta P$, where 10^4 is the number of measurements at each temperature, $P(I_{SW})$ is the probability density for the measured value of the switching current to be I_{SW}, and ΔP is the bin size chosen for plotting the distributions. Figure 7 shows how the effective width of the distribution (i.e., the standard deviation of the measured set of switching currents $\sigma = \sqrt{\sum_{i=1}^{n}\left(I_{SW,i} - \overline{I_{SW}}\right)^2/\left(n-1\right)}$ varies as a function of temperature for samples S1–S5. These samples were fabricated as is illustrated in Figure 1. The only difference between them is that some are made thicker than others and so they exhibit larger critical currents (the values of the critical current are given in the caption to Fig. 7). In this definition, $I_{SW,i}$ represents the 10^4 measured data points for the switching current, whilst $\overline{I_{SW}}$ is the corresponding mean value. We find that (i) the standard deviation (i.e., the fluctuation strength) increases with decreasing

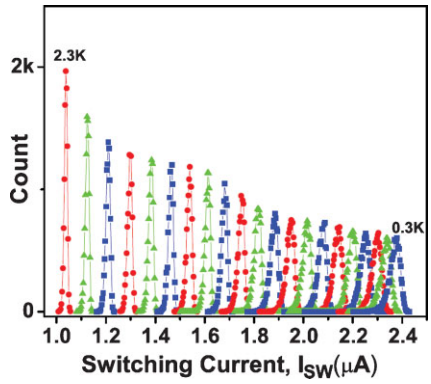

Figure 6. Switching current distributions for sample S1. The distributions are presented for 21 different temperatures in the range between $T = 0.3$ K (right-most peak) and $T = 2.3$ K (left-most peak), with a step size of $\Delta T = 0.1$ K. The parameters of the sample were the length $L = 110$ nm and the normal resistance $R_N = 2.67$ kΩ. To obtain the distribution at each temperature the current was swept 10^4 times, starting from zero up to a value above the switching current. The exact value of the current at which the switching events occurred was recorded for each of the 10^4 sweeps. The histogram is plotted by choosing the bin size to be $\Delta I = 3$ nA. The vertical axis can be expressed as Count $= (10^4)(P(I_{SW}))(\Delta I)$, where 10^4 is the number of measurements and $P(I_{SW})$ is the probability density for the device to switch to the normal state when the bias current has the value I_{SW}.[14]

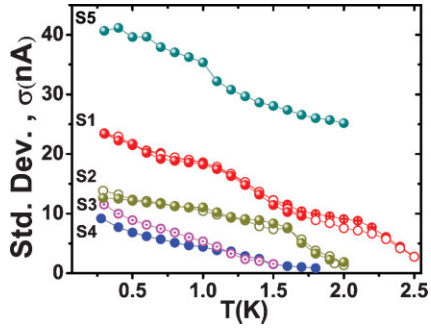

Figure 7. Temperature dependence of the standard deviation of the switching current distribution, plotted versus temperature, for five different samples. The measurements for samples S1 and S2 were repeated more than once, in order to verify their reproducibility. The corresponding values of the critical depairing current for samples S1–S5 are $I_C(0) = 2.92$, 1.72, 1.68, 1.10, and 6.16 μA. The values of the critical current are obtained via a fitting procedure explained in the text.[39,14]

temperature, and (ii) the samples having larger critical currents are characterized by larger values of σ.

It should be emphasized that the observed broadening of the distributions with cooling is, in general, unexpected, as thermal fluctuations, presumably causing the fluctuations in the I_{SW} values, would become weaker with cooling. Note that measurements on SIS Josephson junctions do indeed show just such a trend: the fluctuations became weaker with cooling.[34,35]

5.2. Extracting Switching Rates

Further understanding of the statistics of the switching events can be achieved by applying the analysis of Fulton and Dunkleberger (FD).[35] First, we note that the values of σ introduced above, as well as the exact shape of the $P(I_{SW})$ curves (Fig. 6), are not universal. They depend on the bias-current sweeping rate dI/dt chosen during the measurements of the switching events. The general rule is that: the faster the sweeping rate, the smaller the difference between $\overline{I_{SW}}$ and the depairing current of the wire $I_C = I_C(T)$. In the limit $dI/dt \to \infty$, the premature switching does not have time to happen, and the distribution function becomes a Dirac δ-function centered at $I_C(T)$, namely, $P(I_{SW}) = \delta(I_C(T) - I_{SW})$, and also $\sigma = 0$. The depairing current is the current at which the superconductivity breaks down with certainty because the superconducting state free energy becomes larger than the free energy of the normal state. Therefore, $P(I) = 0$ for $I > I_C(T)$.

The FD analysis allows one to convert the sweep-rate-dependent distribution function $P(I_{SW})$ into the sweep-rate-independent switching rate function $\Gamma(T, I)$. The analysis is based on the relation

$$P(I)dI = \Gamma(I)(dI/dt)^{-1}dI\left(1 - \int_I^0 P(I')dI'\right), \quad (5)$$

where $P(I)dI$ is the probability that the device switches to the normal state in the interval between bias currents I and $I + dI$, $(dI/dT)^{-1}\,dI$ is the duration of time during which the bias current belongs to the interval between I and $I + dI$, $\Gamma(I)$ is the switching rate (i.e., the average number of switching events that the system would undergo if the bias current would be fixed at I), and the expression $\left(1 - \int_0^I P(I')dI'\right) = \int_I^{I_C} P(I')dI'$ gives the probability that the current is swept from zero to I without switching.

In general, the sweeping rate can be a function of the value of the current. For example, if the bias current has a sinusoidal time dependence $I(t) = I_a \sin(\omega t)$ then the sweeping rate is given by, $dI/dT = I_a\omega\cos(\omega t) = \sqrt{1 - (I/I_a)^2}$, where I_a is the amplitude of the bias current, which must satisfy $I_a > I_C(T)$. In the experiment,[14] a triangular sweeping function was used, such that $I_a = 2.75$ μA and $dI/dt = 125.5$ μA s^{-1}.

As, in practice, the histogram is expressed in digital format, the expression for the switching rate needs to be expressed in terms of finite sums rather than integrals. Let the current axis be split into bins of size ΔI and the corresponding current values be numbered $I_k = I_C - k\Delta I$, where the integer bin number k obeys $0 < k < N$, with the highest bin number N defined via $N = I_C/\Delta I$. This type of definition implies that bin number zero corresponds to $I = I_C$ and the higher numbers correspond to lower currents. Then the switching rate can be expressed as:[35]

$$\Gamma_k = \Gamma(I_k) = \frac{dI}{dt}(1/\Delta I)\ln\left(\frac{\sum_{i=0}^{k} P(I_i)}{\sum_{i=0}^{k-1} P(I_i)}\right) \quad (6)$$

5.3. Correspondence Between Switching Events and Phase Slips

The results of the FD-type analysis are shown in Figure 8 for a measurement done at a low temperature, namely, at $T = 300$ mK. The open circles represent the dependence of the switching rate

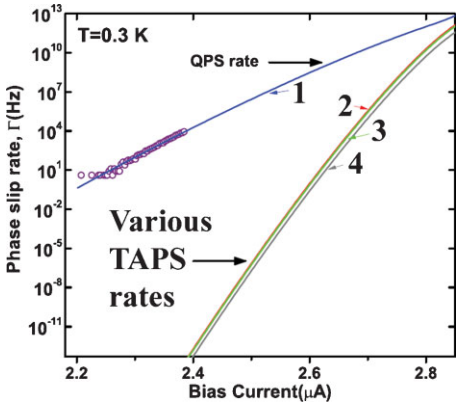

Figure 8. The experimental switching rate (open circles) and the calculated QPS rate (solid blue line) are shown for $T = 0.3$ K for the sample S1. The observed agreement is very good. Various estimates of the TAPS rate by using different attempt-frequency expressions are also shown by solid red, green, and gray lines. For all estimates of the TAPS rate, the experimental values are at least 10^{17} orders of magnitude higher than the calculated thermal rate. Hence, the data cannot be explained by considering thermal fluctuation alone, even if the uncertainty in the attempt frequency is taken into account.[14]

on temperature, and the continuous curves represent different models. The best fit is provided by the QPS model, whilst the models involving only thermal fluctuations and neglecting quantum fluctuations (TAPS models) do not agree with the data at all.

In order to obtain the fits of Figure 8 we have to make an assumption about the relationship between single phase slips (whether thermally activated or quantum) and the switching events observed in the experiment. The simplest assumption is that a single phase slip corresponds to every switching event. Under such hypothesis, as the current is increased the wire initially remains fully superconducting (i.e., it shows zero voltage even though the current is greater than zero) until a single TAPS or QPS occurs. As soon as a single phase slip happens, it dissipates the kinetic energy of the supercurrent in the wire as heat. The heat dissipated as a result of a single LPS is $\Delta E_{\mathrm{LPS}} = hI/2e$. Note that the released heat is proportional to the bias current. A detailed analysis of the heating effect in suspended wires, due to Shah et al.,[36] shows that if the temperature is sufficiently low (and $T = 300$ mK was sufficiently low for our samples), the dissipated energy ΔE is sufficient to increase the temperature of the wire above its current-dependent critical temperature $T_{\mathrm{C}}(I)$. To understand why at low temperatures a single LPS is sufficient to increase the temperature of the wire above $T_{\mathrm{C}}(I)$ while at higher temperatures a single LPS is not sufficient we first remind the fact that LPSs are less frequent at low temperatures for a given value of the LPS barrier. Thus, as the current is slowly increased, the wire stays LPS-free until the current is very near the depairing current. Therefore, the first phase slip occurs when ΔE_{LPS} is high and $T_{\mathrm{C}}(I)$ is low, so just one LPS is sufficient to overheat the wire above the current-dependent critical temperature. At sufficiently higher temperatures the LPS start to occur with an appreciable frequency, even at a low bias current at which $E_{\mathrm{LPS}} = hI/2e$ is still low and $T_{\mathrm{C}}(I)$ is high. Thus one LPS cannot overheat the wire. If overheating happens, the wire becomes normal, at least for a short time, until the dissipated heat has enough time to flow away from the nanowire (this typically takes some nanoseconds). As the current through the wire I is set by an external current source, the current keeps flowing even if an LPS makes it temporarily nonsuperconducting. The additional Joule heating generated due to the current passing through a nonsuperconducting region of the wire leads to further, rapid growth of the temperature, which eventually leads to the observable switching event. Thus, the statistics of the switching events is in one-to-one correspondence with the statistics of phase slips—at low enough temperatures when a single LPS can make a small segment of the wire normal, at least for a short period of time. In order to explain these stochastic features quantitatively, we review below the formulas describing the rates of QPS and TAPS.

5.4. Rates of Phase Slips

The rate of TAPS is given by the Arrhenius-type expression[21]

$$\Gamma_{\mathrm{TAPS}} = (\Omega_{\mathrm{TAPS}}/2\pi)\exp(-\Delta F/k_{\mathrm{B}}T) \tag{7}$$

By analogy, the rate of QPSs can be estimated as

$$\Gamma_{\mathrm{QPS}} = (\Omega_{\mathrm{QPS}}/2\pi)\exp(-\Delta F/k_{\mathrm{B}}T_{\mathrm{Q}}) \tag{8}$$

which was justified by Giordano[19] and Lau et al.[37] Here, T_{Q} is an effective temperature characterizing the strength of quantum fluctuations.[34] If the device under consideration contains a superconducting wire that links two macroscopic electrodes (as is the case in the experiments discussed in the Research News), the kinetic inductance of the wire is given by[38] $L_{\mathrm{K}} = (L/\xi(T))\hbar/3\sqrt{3}eI_{\mathrm{C}}$, and the electrical capacitance between the electrodes is C_{E}, then the quantum temperature can be roughly estimated as $T_{\mathrm{Q}} = (\hbar/k_{\mathrm{B}})/\sqrt{L_{\mathrm{K}}C_{\mathrm{E}}}$

To analyze data at temperatures well below T_{C}, we estimate the barrier for phase slips by combining Equation (2–4). The result is a formula that is valid, to a good approximation, over a wide temperature range:

$$\Delta F(T) = \left(\sqrt{6}(\hbar/2e)\right)0.83k_{\mathrm{B}}T_{\mathrm{C}}\left(R_{\mathrm{Q}}/R_{\mathrm{N}}\right)(L/\xi(0)) \times \left(1-(T/T_{\mathrm{C}})^2\right)^{3/2} \tag{9}$$

In order to make fits to the experimentally obtained switching rates, one needs to know how the barrier for the LPS changes with the bias current. The corresponding formula is[17]

$$\Delta F(I,T) = \Delta F(0,T)(1-I/I_{\mathrm{C}}(T))^{5/4} \tag{10}$$

where $\Delta F(0, T)$ is the barrier energy to phase slip at zero current and a given temperature. It is worth noting that the corresponding expression for the more thoroughly studied case of a Josephson junction has the same form,[21] but an exponent of 3/2 instead of 5/4. Qualitatively, the two cases are very similar.[17]

The attempt frequency for the QPS can be plausibly estimated from the LAMH attempt frequency, Equation (1), by replacing the thermal energy k_BT by an effective quantum energy. In Reference [14] the choice was made to make the following replacement in the LAMH expression for the attempt frequency: $\Delta F/k_BT \rightarrow \Delta F/k_BT_Q$. There is no rigorous justification for such replacement. But, fortunately, the choice of the attempt frequency is not important, as the expression for the switching rate is always dominated by the exponential factor, as we shall discuss below. The QPS attempt frequency thus becomes:

$$\Omega_{QPS} = (8k_B(T_C - T)/\pi\hbar)(L/\xi(T))\sqrt{\pi\Delta F(T)/k_BT_Q} \quad (11)$$

The QPS switching rate computed using Equation (8–11) is plotted in Figure 8 versus the bias current (see the blue curve, marked 1). The fitting parameters used are $T_Q = 0.85$ K, $T_C = 3.87$ K, and $\xi(0) = 5$ nm. The parameters known from independent measurements are the normal resistance and the sample length, namely, $R_N = 2.67\ k\Omega$ and $L = 110$ nm. The calculated rate is in a good agreement with the data. Thus, the hypothesis that QPS control the observed strong fluctuations of the switching current finds significant justification. Additional justification comes from the fact that T_Q was observed to become greater in wires of larger diameter, which have higher critical currents.[14] If the observed strong fluctuations of I_{SW} were due to some trivial reason, such as an excess electromagnetic noise in the setup leads, or granularity in the wires, then one would expect to see a smaller T_Q in thicker wires. This is because thicker wires would, presumably, be less susceptible to problems such as electromagnetic noise or granularity of the wire. In reality, larger T_Q values were found in thicker wires.[14]

On the other hand, curves 2–4 (see Fig. 8) all represent the TAPS model, given by Equation (7). The reason we show three curves is that in this model the attempt frequency is not well established, except very near T_C.[22] In the case of curve 2, LAMH theory was followed and the assumption was made that $\Omega_{TAPS} = \Omega_{LAMH}$ (see Eq. (1)). Curve 3 (green) is plotted using a modified attempt frequency. The new expression is obtained by using Equation (1) and replacing $1/\tau_{GL}$ with ω_p, where $\omega_p = \sqrt{2eI_C(T)/\hbar C_E}$ is the so-called plasma frequency of a Josephson junction. Curve 4 (gray) is again obtained using Equation (1) but this time replacing $1/\tau_{GL}$ with ω_w, where $\omega_w = 1/\sqrt{L_K C_E}$ is the analog of the plasma frequency for a system having a nanowire. Apparently, none of the TAPS expressions tested can fit the data. Also it is clear that the exponential factor dominates over the pre-exponential attempt frequency. In other words, any tested choice of the attempt frequency gives almost the same result: the curves 2–4 are very close to one another. This gives evidence that, as with TAPS, the choice of the attempt frequency for QPS is not essential and need not be known precisely.

Finally, a general model was developed, which takes into account both TAPS and QPS. The model also takes into account the fact that at higher temperatures a single LPS is not sufficient to cause a switching event.[14,36] On the contrary, the model predicts that, at higher temperatures, many phase slips must occur almost simultaneously in order to overheat the wire and switch it into the JNS.[14,36] This conclusion is directly confirmed by the fact that the $V(I)$ curves measured at higher temperatures (i.e., close to T_C) show nonzero voltages before the switch to the JNS occurs. For example, on sample S1 such a pre-switching voltage tail was observed down to $T \sim 2.5$ K.[14] This fact confirms that LPSs occur before the switch. The results of the general model, in comparison to the experiment, are shown in Figure 9. In Figure 9a the experimental switching rate was compared to a partial model, which includes only TAPS. It is clear that the model of overheating with TAPS works well at higher temperatures, but fails to describe data below $T \sim 1$ K. Thus, one needs to bring QPS into consideration. The fitting curves in Figure 9b are computed by including both the TAPS and QPS switching rates. In this case, good agreement is observed over the entire temperature interval, down to $T = 0.3$ K. Thus, it is clear that the phenomenon of MQT must be included in the model in order to obtain reasonable agreement with the data. We also note that the general overheating model[36] provides a natural explanation of the observed growth, as the temperature is reduced, in the fluctuations of I_{SW} (see Fig. 7). The explanation is that a smaller and smaller number of LPSs is required to overheat the wire as the temperature is reduced. Thus, the stochastic nature of the switching process becomes more pronounced.

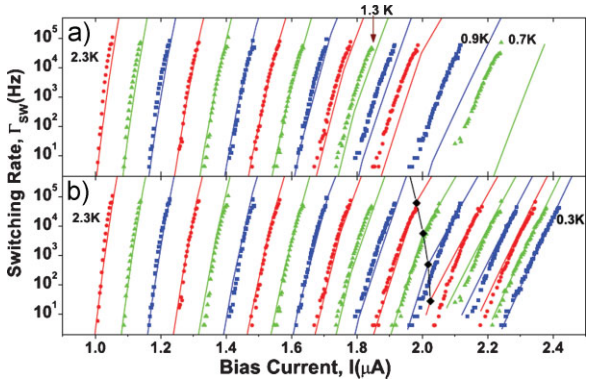

Figure 9. a) Switching rates from the superconducting state to the resistive state for bath temperatures between 2.3 K (left most) and 0.7 K (right most). (For the sake of clarity, not all the measured curves are shown here.) The data are shown for all temperatures between 2.3 and 1.1 K with $\Delta T = 0.1$ K as well as for $T = 0.9$ K and $T = 0.7$ K (sample S1). The symbols are experimental data and the lines (with corresponding colors) are fits to the overheating model, incorporating stochastic TAPS-only events.[14,36] The fits agree well with the data down to $T = 1.3$ K, which is indicated by an arrow. b) Fits to the same data (all temperatures are shown here) with the stochastic overheating model but now incorporating both TAPS and QPS rates. The boundary for the single phase-slip-switching regime is indicated by the black diamond symbols, connected by line segments, for four temperatures. The single-phase-slip switching regime occurs to the right of the line connecting the diamonds.[39]

6. Summary

In this Research News article we have covered three main topics: i) the molecular templating technique for making nanowires, ii) the transport properties of molecule-templated superconducting nanowires, and iii) evidence for the occurrence of MQT in nanowires at high values of the supercurrent.

The best molecules for fabricating nanowires turn out to be fluorinated single-walled carbon nanotubes. DNA has the disadvantage of being less rigid, compared to carbon nanotubes. Also, nanowires made with DNA tend to be somewhat larger in diameter, possibly because the DNA molecule has a larger diameter after being suspended and dried, due to the difficulty of removing all contamination surrounding the molecule. The potential advantage of DNA molecules, associated with their ability to self-assemble into complex constructs with pre-designed geometries, has not, to date, been realized and employed for the fabrication of superconducting networks (except DNA-templated nanowire SQUIDS having two nanowires in parallel).[7,8] This possibility remains for future research on molecule-templated devices. The idea would be to design and synthesize DNA molecules of well-defined sequences of base pairs, and to then allow these molecules to self-assemble into a network with a desired structural configuration.[40] It is expected that such networks can be formed in a suspended state and then coated with superconducting metal or alloy. Thus, a network of ultrathin superconducting wires would be obtained. Such superconducting wire networks could be used for information processing, where the information bits are represented by different values of quantized supercoducting currents circulating around the cells of the network.

Transport measurements on thin superconducting wires confirmed the expected absence of a thermodynamic normal-to-superconductor phase transition. This absence is explicitly manifested by the fact the the resistance remains greater than zero at any nonzero temperature (although it does become smaller with cooling and can fall below the sensitivity of the experimental setup). The resistance is governed by the Arrhenius law of thermal activation, the energy barrier of which is determined by the free energy required to convert a segment of the wire from the superconducting to the normal state.

Proving that MQT does indeed occur in thin superconducting wires is a formidable task. The difficulties arise because other factors can be easily mistaken for MQT. Our approach for showing the existence of MQT is based on a trigger effect that is related to the Joule-overheating of the wires. When a single phase-slip occurs, the temperature of the wire jumps, switching the wire to the normal state. Such switching events are easy to detect, in contrast with individual phase slips. The proof of the existence of MQT is based on our observations (i) that the fluctuations of the switching current are much larger than would be expected on the basis of thermal fluctuations at a given temperature, and (ii) that the observed fluctuations are larger in wires that have larger critical currents.

In the future, we plan to continue studies of MQT effects in thin wire devices. The next step will be to employ an environmental dissipation bath, possibly represented by a normal resistor, in order to control the rate of QPS, following the general ideas set forth by Leggett.[27]

Acknowledgements

The authors gratefully acknowledge many extensive and highly informative discussions on the topics reviewed here (as well as on related issues), which they have enjoyed with their colleagues and collaborators, especially D. Hopkins, A. J. Leggett, D. Pekker, G. Refael, A. Rogachev, M. Sahu, N. Shah, and T.-C. Wei. They also gratefully acknowledge the use of fabrication facilities at the Frederick Seitz Materials Research Laboratory. This material is based upon work supported by the U.S. Department of Energy, Division of Materials Sciences under Award No. DE-FG02-07ER46453, through the Frederick Seitz Materials Research Laboratory at the University of Illinois at Urbana-Champaign. This article is part of a Special Issue on Materials Research at the Frederick Seitz Materials Research Laboratory.

Received: December 18, 2009
Published online: March 1, 2010

[1] A. Bezryadin, C. N. Lau, M. Tinkham, *Nature* **2000**, *404*, 971.
[2] A. T. Bollinger, R. C. Dinsmore, A. Rogachev, A. Bezryadin, *Phys. Rev. Lett.* **2008**, *101*, 227003.
[3] Y. Zhang, H. Dai, *Appl. Phys. Lett.* **2000**, *77*, 3015.
[4] A. Bezryadin, A. Bollinger, D. Hopkins, M. Murphey, M. Remeika, A. Rogachev, in *Dekker Encyclopedia of Nanoscience and Nanotechnology* (Eds: J. A. Schwarz, C. I. Contescu, K. Putyera), Marcel Dekker, Inc., New York **2004**, p. 3761.
[5] M. Remeika, A. Bezryadin, *Nanotechnology* **2005**, *16*, 1172.
[6] A. Bezryadin, *J. Phys.: Condens. Matter* **2008**, *76*, 43202.
[7] D. Hopkins, D. Pekker, P. Goldbart, A. Bezryadin, *Science* **2005**, *308*, 1762.
[8] D. S. Hopkins, D. Pekker, T.-C. Wei, P. M. Goldbart, A. Bezryadin, *Phys. Rev. B, Rapid Commun.* **2007**, *76*, 220506(R).
[9] A. Rogachev, A. Bezryadin, *Appl. Phys. Lett.* **2003**, *83*, 512.
[10] J. M. Graybeal, M. R. Beasley, *Phys. Rev. B* **1984**, *29*, 4167.
[11] J. M. Graybeal, *PhD Thesis*, Stanford 1985.
[12] W. A. Little, *Phys. Rev.* **1967**, *156*, 396.
[13] K. Xu, J. R. Heath, *Nano Lett.* **2008**, *8*, 3845.
[14] M. Sahu, M.-H. Bae, A. Rogachev, D. Pekker, T.-C. Wei, N. Shah, P. M. Goldbart, A. Bezryadin, *Nat. Phys.* **2009**, *5*, 503.
[15] A. Bezryadin, C. Dekker, *J. Vac. Sci. Technol, B* **1997**, *15*, 793.
[16] Y. Oreg, A. M. Finkel'stein, *Phys. Rev. Lett.* **1999**, *83*, 191.
[17] M. Tinkham, J. U. Free, C. N. Lau, N. Markovic, *Phys. Rev. B* **2002**, *68*, 134515.
[18] D. E. McCumber, B. I. Halperin, *Phys. Rev. B* **1970**, *1*, 1054.
[19] N. Giordano, *Phys. Rev. Lett.* **1988**, *61*, 2137.
[20] J. S. Langer, V. Ambegaokar, *Phys. Rev.* **1967**, *164*, 498.
[21] M. Tinkham, *Introduction to Superconductivity*, 2nd ed., McGraw-Hill, New York **1996**.
[22] D. Meidan, Y. Oreg, G. Refael, *Phys. Rev. Lett.* **2007**, *98*, 187001.
[23] S. L. Chu, A. T. Bollinger, A. Bezryadin, *Phys. Rev. B* **2004**, *70*, 214506.
[24] M. Tinkham, C. N. Lau, *Appl. Phys. Lett.* **2002**, *80*, 2946.
[25] J. Bardeen, *Rev. Mod. Phys.* **1962**, *34*, 667.
[26] M. Arndt, O. Nairz, J. Voss-Andreae, C. Keller, G. van der Zouw, A. Zeilinger, *Nature* **1999**, *401*, 680.
[27] a) A. J. Leggett, *J. Phys. Colloq.* **1978**, *39*, 1264; A. J. Leggett, *Prog. Theor. Phys. Suppl.* **1980**, *69*, 80. b) A. O. Caldeira, A. J. Leggett, *Phys. Rev. Lett.* **1981**, *46*, 211. c) A. J. Leggett, S. Chakravarty, A. T. Dorsey, A. Garg, W. Zwerger, *Rev. Mod. Phys.* **1987**, *59*, 1.
[28] a) R. F. Voss, R. A. Webb, *Phys. Rev. Lett.* **1981**, *47*, 265. b) K. Inomata, S. Sato, K. Nakajima, A. Tanaka, Y. Takano, H. B. Wang, M. Nagao, H. Hatano, S. Kawabata, *Phys. Rev. Lett.* **2005**, *95*, 107005. c) A. Wallraff, A. Lukashenko, J. Lisenfeld, A. Kemp, M. V. Fistul, Y. Koval, A. V. Ustinov, *Nature* **2003**, *425*, 155.
[29] W. Wernsdorfer, E. Bonet Orozco, K. Hasselbach, A. Benoit, D. Mailly, O. Kubo, H. Nakano, B. Barbara, *Phys. Rev. Lett.* **1997**, *79*, 4014.
[30] a) P. Shor, Proc. 35th Annual Symposium on Foundations of Computer Science, 1994, pp. 124–134. b) P. Shor, *SIAM J. Comput.* **1997**, *26*, 1484.
[31] A. Izmalkov, M. Grajcar, E. IlŠichev, Th. Wagner, H.-G. Meyer, A. Yu. Smirnov, M. H. S. Amin, A. M. van den Brink, A. M. Zagoskin, *Phys. Rev. Lett.* **2004**, *93*, 037003.
[32] J. E. Mooij, C. J. P. M. Harmans, *New J. Phys.* **2005**, *7*, 219.
[33] K. Yu. Arutyunov, D. S. Golubev, A. D. Zaikin, *Phys. Rep.* **2008**, *464*, 1.

[34] a) J. M. Martinis, M. H. Devoret, J. Clarke, *Phys. Rev. B* **1987**, *35*, 4682. b) J. R. Friedman, V. Patel, W. Chen, S. K. Tolpygo, J. E. Lukens, *Nature* **2000**, *406*, 43.
[35] T. A. Fulton, L. N. Dunkleberger, *Phys. Rev. B* **1974**, *9*, 4760.
[36] a) N. Shah, D. Pekker, P. M. Goldbart, *Phys. Rev. Lett.* **2008**, *101*, 207001. b) D. Pekker, N. Shah, M. Sahu, A. Bezryadin, P. M. Goldbart, *cond-mat. supr-con* **2009**, arXiv:0904.4432v1.
[37] C. N. Lau, N. Markovic, M. Bockrath, A. Bezryadin, M. Tinkham, *Phys. Rev. Lett.* **2001**, *87*, 217003.
[38] K. K. Likharev, *Rev. Mod. Phys.* **1979**, *51*, 101.
[39] M. Sahu, *PhD Thesis*, University of Illinois at Urbana-Champaign **2009**.
[40] a) P. W. Rothemund, *Nature* **2006**, *440*, 297. b) E. S. Andersen, M. Dong, M. M. Nielsen, K. Jahn, R. Subramani, W. Mamdouh, M. M. Golas, B. Sander, H. Stark, C. L. Oliveira, J. S. Pedersen, V. Birkedal, F. Besenbacher, K. V. Gothelf, J. Kjems, *Nature* **2009**, *459*, 73. c) F. A. Aldaye, A. L. Palmer, H. F. Sleiman, *Science* **2008**, *321*, 1795. d) E. Braun, K. Keren, *Adv. Phys.* **2004**, *53*, 441. e) H. Watanabe, C. Manabe, T. Shigematsu, K. Shimotani, M. Shimizu, *Appl. Phys. Lett.* **2001**, *79*, 2462. f) N. C. Seeman, *Angew. Chem. Int. Ed.* **1998**, *37*, 3220. g) E. Braun, Y. Eichen, U. Sivan, G. Ben-Yoseph, *Nature* **1998**, *391*, 775. h) J. Richter, M. Mertig, W. Pompe, I. Monch, H. K. Schakert, *Appl. Phys. Lett.* **2001**, *78*, 536.